Ground-state and pairing-vibrational bands with equal quadrupole collectivity in ¹²⁴Xe

A.J. Radich, ^{1,*} P.E. Garrett, ¹ J.M. Allmond, ² C. Andreoiu, ³ G.C. Ball, ⁴ L. Bianco, ^{1,†} V. Bildstein, ¹ S. Chagnon-Lessard, ^{1,‡} D.S. Cross, ³ G.A Demand, ¹ A. Diaz Varela, ¹ R. Dunlop, ¹ P. Finlay, ^{1,§} A.B. Garnsworthy, ⁴ G. Hackman, ⁴ B. Hadinia, ¹ B. Jigmeddorj, ¹ A.T. Laffoley, ¹ K.G. Leach, ^{1,¶} J. Michetti-Wilson, ¹ J.N. Orce, ^{4,5} M.M. Rajabali, ^{4,**} E.T. Rand, ¹ K. Starosta, ³ C.S. Sumithrarachchi, ^{1,††} C.E. Svensson, ¹ S. Triambak, ^{4,5,6} Z.M. Wang, ^{3,4} J.L. Wood, ⁷ J. Wong, ¹ S.J. Williams, ^{4,††} and S.W. Yates ¹ Department of Physics, University of Guelph, Guelph, ON, N1G2W1, Canada ² Physics Division, Oak Ridge National Laboratory, Oak Ridge, TN 37831, USA

²Physics Division, Oak Ridge National Laboratory, Oak Ridge, TN 37831, USA

³Department of Chemistry, Simon Fraser University, Burnaby, BC, V5A1S6, Canada

⁴TRIUMF, 4004 Wesbrook Mall, Vancouver, BC, V6T 2A3, Canada

⁵Department of Physics, University of the Western Cape, P/B X17, Bellville ZA-7535, South Africa

⁶iThemba LABS, P.O. Box 722, Somerset West 7129, South Africa

⁷School of Physics, Georgia Institute of Technology, Atlanta, GA 30332-0430, USA

⁸Departments of Chemistry and Physics & Astronomy,

University of Kentucky, Lexington, KY 40506-0055, USA

(Dated: February 2, 2015)

The nuclear structure of 124 Xe has been investigated via measurements of the β^+/EC decay of 124 Cs with the 8π γ -ray spectrometer at the TRIUMF-ISAC facility. The data collected have enabled branching ratio measurements of weak, low-energy transitions from highly excited states, and the $2^+ \to 0^+$ in-band transitions have been observed. Combining these results with those from a previous Coulomb excitation study, $B(E2; 2_3^+ \to 0_2^+) = 78(13)$ W.u. and $B(E2; 2_4^+ \to 0_3^+) = 53(12)$ W.u. were determined. The 0_3^+ state, in particular, is interpreted as the main fragment of the proton-pairing vibrational band identified in a previous $^{122}\text{Te}(^3\text{He},n)^{124}\text{Xe}$ measurement, and has quadrupole collectivity equal to, within uncertainty, that of the ground-state band.

PACS numbers: 21.10.-k,21.10.Re,23.20.-g,23.20.Lv,23.20.-s

Nuclei in the Z > 50, N < 82 region (i.e. north-west of ¹³²Sn) display a remarkably smooth evolution of their properties. As highlighted by Rowe and Wood [1], this region is unsurpassed in the smoothness of the trends in the first 2^+ energy and $B(E2; 2_1^+ \rightarrow 0_1^+)$ values, with no abrupt changes observed. It is thus an ideal region in which to explore the development of collectivity progressing away from the doubly-magic ¹³²Sn towards the well-deformed mid-shell. This region is also the focus of many searches for a possible neutrinoless double- β decay mode $0\nu\beta\beta$. Observation of this process would reveal the nature of the neutrino as a Majorana particle, while a measurement of the rate would provide information on the Majorana mass of the neutrino provided that the nuclear-structure-dependent matrix element is known [2]. Some of the most promising candidates in which to pursue observation of the $0\nu\beta\beta$ process include

 $^{130}\mathrm{Te}$ (see, e.g., Ref. [3]), $^{136}\mathrm{Xe}$ (see, e.g., Ref. [4]), and $^{124}\mathrm{Sn}$ [2], and for the double-electron-capture $0\nu\mathrm{ECEC}$ mode, $^{124}\mathrm{Xe}$ [5, 6].

Motivated by the need to evaluate the nuclear matrix elements for the $0\nu\beta\beta$ mode, there has been a renewed interest in using transfer reactions to probe the occupancies and correlations of the protons and neutrons involved [7]. Especially important are the results of twonucleon transfer (TNT) experiments on even-even nuclei where the transfer strength is shared by the ground and excited 0⁺ states indicating a departure from BCStype wave functions [7]. Strong transitions observed in TNT reactions to excited 0⁺ states can arise from gaps in the single-particle spectrum leading to pairing vibrations, shape coexistence, and pairing isomers. In the absence of other complementary data, the observation of strong TNT transitions alone is insufficient information to determine the nature of the 0^+ wave function. In the Cd region, there is convincing evidence, including strong enhancements in the $(^{3}\text{He},n)$ two-proton transfer cross sections to excited 0⁺ states [8], that the shapecoexisting intruder bands are based on proton 2p-2hexcitations (resulting in a 2p-4h configuration) across the Z = 50 closed shell. The interaction of the additional proton 2 valence particles and 2 valence holes with the neutrons in the open 50-82 shell and the gain in the correlation energy results in the appearance of the deformed rotational-like band in the low-excitation energy region [9-12]. Thus, the shape-coexisting states in the near-to-mid shell Cd isotopes are the main fragments of

^{*} e-mail: aradich@uoguelph.ca

 $^{^\}dagger$ Present address: DESY Photon Science, Notkestrasse 85 D-22607 Hamburg, Germany

[‡] Present address: Department of Physics, University of Ottawa, 150 Louis-Pasteur, Ottawa, ON K1N 6N5, Canada

[§] Present address: Instituut voor Kern-en Stralingsfysica, K.U. Leuven, Celestijnenlaan 200D, B-3001 Leuven, Belgium

[¶] Present address: TRIUMF, 4004 Wesbrook Mall, Vancouver, BC, V6T 2A3, Canada

^{**} Present address: Department of Physics, Tennessee Technological University, Cookeville, TN 38505, USA

 $^{^{\}dagger\dagger}$ Present address: National Superconducting Cyclotron Laboratory, Michigan State University, East Lansing, MI 48824, USA

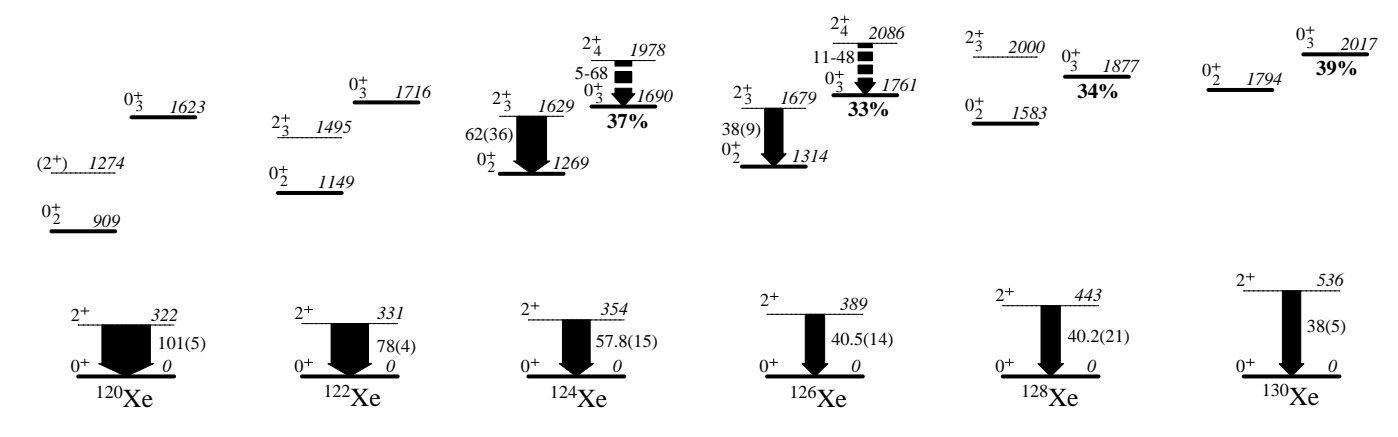


FIG. 1. Systematics of the low-lying 0^+ states in the 120 Xe $^{-130}$ Xe isotopes. Absolute in-band $B(E2; 2^+ \to 0^+)$ values are shown, where known [16–18], in W.u. with uncertainties in parentheses. The possible ranges of values for the 0_3^+ bands in 124 Xe and 126 Xe were derived from Coulomb excitation analyses [17, 18] for these unobserved transitions. For $^{124-130}$ Xe, the values of the ratio of the (3 He,n) cross section attributed to the 0_3^+ state to that of the ground state are written below the 0_3^+ levels in percentages [15, 19].

the proton-pairing vibrational states.

The $(^{3}\text{He},n)$ reaction on the tin isotopes [13] also showed enhancements to excited 0^+ states in the Te isotopes, but unlike the mid-shell Cd isotopes, to date there has been no convincing evidence of a shape-coexisting band based on these 0^+ states. (Rotational bands have been observed in the lighter-mass Te isotopes (see, e.g. Ref. [14]), but none extended down to a 0^+ band head.) The $Te(^3He,n)$ two-proton transfer reactions populating the Xe isotopes [15] also located the low-lying fragment of the proton-pairing vibration, with a 0^+ state between $1.65~\mathrm{MeV}~(^{124}\mathrm{Xe})$ and $2.1~\mathrm{MeV}~(^{130}\mathrm{Xe})$ populated with approximately 1/3 of the ground-state strength. Figure 1 summarizes the systematics of the low-lying excited 0⁺ states in the ¹²⁰Xe-¹³⁰Xe isotopic chain. The in-band $B(E2; 2^+ \rightarrow 0^+)$ values, in W.u., are shown where known [16-18]. Displayed under the 0_3^+ levels are the (${}^3\mathrm{He},n$) cross sections [15] relative to that of the ground state [19]. As Fig. 1 shows, the $B(E2; 2^+ \to 0^+)$ values in the pairing-vibrational band in 124,126Xe have such large uncertainties that their degree of quadrupole collectivity is difficult to assess.

Recently, the stable Xe isotopes have been the subject of detailed Coulomb excitation studies [17, 18, 20, 21] with beams of the Xe isotopes bombarding a 12 C target and the resulting de-excitation γ rays detected using the GAMMASPHERE array. These experiments provided a wealth of information on matrix elements, and allowed detailed tests of nuclear structure models [17, 18, 20] and the elucidation of the evolution of mixed-symmetry states [21]. The study [17] of 124 Xe, in particular, provided numerous B(E2) transition strengths for off-yrast, low-spin states. The results were compared with Interacting Boson Model (IBM) calculations and indicated that 124 Xe badly breaks O(6), but preserves O(5) symmetry [17].

As shown in Fig. 1, in 124 Xe there were two key transitions for which the matrix elements could not be ac-

curately determined: the $2_3^+ \to 0_2^+$ and the $2_4^+ \to 0_3^+$ transitions. These transitions represent the in-band decays and an accurate measurement of their B(E2) values is crucial in determining the quadrupole collectivity of the bands. The 289-keV $2_4^+ \to 0_3^+$ transition, in fact, has never been observed in any experiment to date for 124 Xe, but its existence was hypothesized using γ -ray yields of other observed decay branches [17]. Observation of these missing transitions and measurements of their B(E2) values would provide the information needed to further investigate the structure of this nucleus. Experiments utilizing β decay are ideal to search for such weak γ -decay branches that are often unobserved with other experimental techniques.

An experiment to observe low-energy, weak decay branches in ¹²⁴Xe was performed at the Isotope Separator and Accelerator (ISAC) facility at TRIUMF in Vancouver, Canada. A 25- μ A beam of 500-MeV protons from the TRIUMF main cyclotron bombarded a thick tantalum production target, inducing spallation reactions. The reaction products diffused through the target and were surface ionized and mass separated to produce a beam containing 9.8×10^7 ions/s $^{124}\mathrm{Cs}$ ($J^{\pi}=1^+$, $T_{1/2}=30.8$ s) and 2.6×10^6 ions/s $^{124}\mathrm{Cs}^m$ ($J^{\pi}=(7)^+$, $T_{1/2}=6.3$ s). The beam was implanted into a moveable mylar-backed FeO tape in the center of the $8\pi \gamma$ ray spectrometer – an array of 20 Compton-suppressed high-purity germanium detectors in a truncated icosahedral arrangement [22]. The tape system was operated in a cycling mode. Singles γ -ray and γ - γ coincidence data were collected during the implantation and decay period, after which the implantation site was transported behind a thick lead wall to remove any long-lived sources from the focal volume of the 8π array. The following cycle times were implemented: 5 s of implantation and 6 s of decay for 8 hours; 1 s of implantation and 12 s of decay for 8 hours; and 300 s of implantation and 45 s of decay

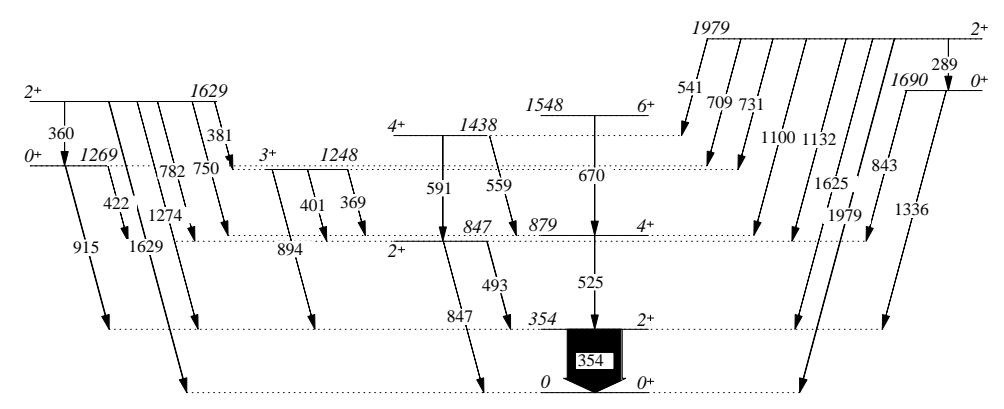


FIG. 2. Partial level scheme observed in the $\beta^+/\text{EC-decay}$ of $^{124}\text{Cs.}$ Levels are labelled with their energies in keV, and their J^π values. The transitions are labelled with their energies in keV, with arrow widths proportional to the observed intensity.

for 35 hours. Calibration measurements using sources of 152 Eu, 56 Co, 60 Co and 133 Ba were performed immediately following the experiment. The data were sorted into a time-random-background subtracted γ - γ coincidence matrix containing approximately 4.5×10^8 events and analyzed with the Radware package of programs [23].

The analysis procedure was outlined in Ref. [24, 25]. Briefly, all branching ratios were determined by analyzing coincidence-gated γ -ray spectra, generally by taking the coincidence gate from below. The number of counts in a coincidence peak, N_c , is given by

$$N_c = \mathcal{N}I_{\gamma}^f \epsilon_{\gamma}^f B R_{\gamma}^d \epsilon_{\gamma}^d \epsilon_c \eta(\theta_{fd}) \tag{1}$$

where \mathcal{N} is an overall normalization factor for a particular data set, I_{γ} is the γ -ray intensity for the feeding f or draining d transition from a level, BR_{γ}^{d} is the branching ratio of the draining transition, ϵ_{γ} is the γ -ray detection efficiency, ϵ_{c} accounts for the deviation of the relative efficiency from that determined using singles analysis due to the coincidence condition, which in principle depends on

both the feeding and draining γ -ray energies, and $\eta(\theta_{fd})$ is the angular correlation correction factor for the particular pair of feeding and draining γ rays. Angular correlation effects are generally smaller than a few percent due to the symmetry of the 8π spectrometer [26]. To account for such effects, in addition to the statistical uncertainties of the γ -ray peak areas, a 3% systematic uncertainty was added in quadrature to the relative intensities of the γ rays. The γ - γ coincidence efficiency factor ϵ_c is generally most affected by timing conditions placed on the data and since these were very generous ($|\Delta t_{\gamma\gamma}| \leq 200$ ns), it was assumed to be 1. The validity of this assumption was verified by branching ratios obtained using multiple gates and comparison with singles intensities [25]. To generate the coincidence spectra, generally the gate was taken on the strongest draining transition. Intensities were obtained by dividing the peak area by the γ -ray singles photopeak efficiencies of both the feeding and draining γ rays and the branching ratio of the draining γ ray. Branching ratios were then found by dividing

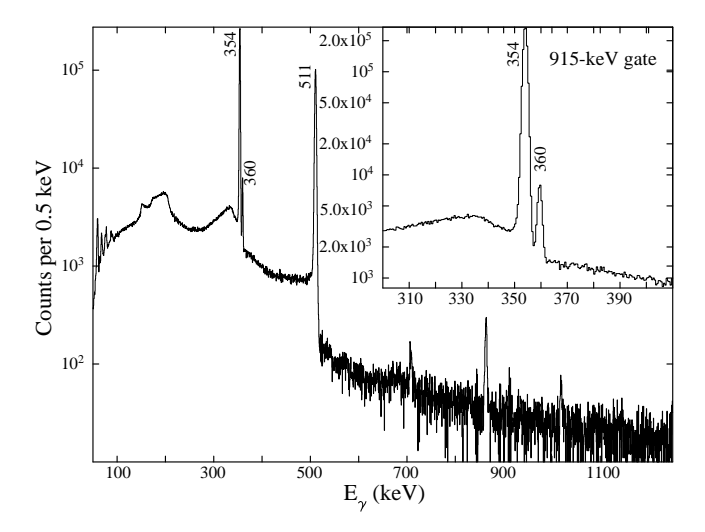


FIG. 3. Portion of the γ -ray coincidence spectrum gated on the 915-keV $0_2^+ \to 2_1^+ \gamma$ ray showing the 360-keV γ ray from the 1629-keV level. The inset displays an expanded region of the spectrum centered near 350 keV.

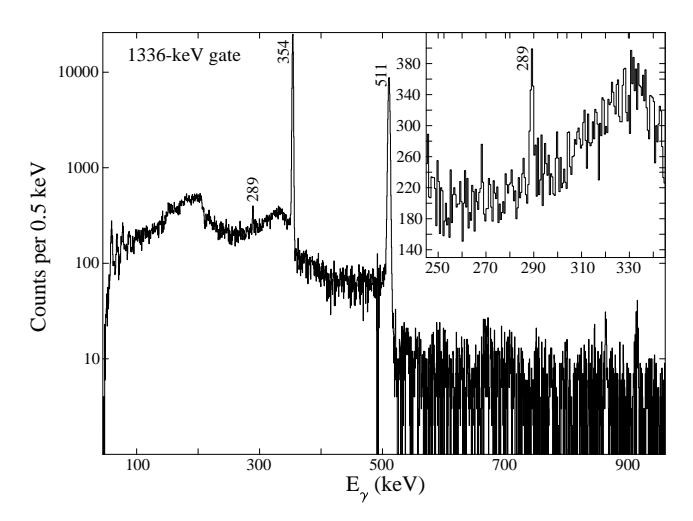


FIG. 4. Portion of the γ -ray coincidence spectrum gated on the 1336-keV $0_3^+ \rightarrow 2_1^+ \gamma$ ray showing the 289-keV γ ray from the 1979-keV level. The inset displays an expanded region of the spectrum centered near 290 keV.

TABLE I. Experimental data for the low-lying " $K^{\pi} = 0^{+}$ " bands in ¹²⁴Xe. The previous results are those from Ref. [17]. Energies are given in keV and B(E2) values in W.u. (uncertainties are given in parentheses) with those indicated by an asterisk used as the reference transition in Eq. 2. The rightmost columns are predictions using the IBM [17], and the DPPQ model [28].

State	Experimental						Theoretical			
	E_{ex}	$I_i^\pi \to I_f^\pi$	Previous		Present		IBM		DPPQ	
			BR	B(E2)	BR	B(E2)	E_{ex}	B(E2)	E_{ex}	B(E2)
2_1^+	354	$2_1^+ \to 0_1^+$	1.0	57.8(15)	1.0		354		355	62
2_2^+	847	$2_{2}^{+} \rightarrow 2_{1}^{+} 2_{2}^{+} \rightarrow 0_{1}^{+}$	0.750(2) 0.250(2)	$64(5) \\ 1.45(12)$	$0.774(12) \\ 0.226(12)$	74(7)	811	61 1.47	1097	$45 \\ 0.03$
0_{2}^{+}	1269	$0_2^+ \to 2_2^+ \ 0_2^+ \to 2_1^+$	$0.122(12) \\ 0.878(12)$	$87(21) \\ 13.2(31)$	0.098(4) 0.902(4)	68(16) *	1104	76 16	1099	82 57
2_3^+	1629	$\begin{array}{c} 2^{+}_{3} \rightarrow 0^{+}_{2} \\ 2^{+}_{3} \rightarrow 3^{+}_{1} \\ 2^{+}_{3} \rightarrow 4^{+}_{1} \\ 2^{+}_{3} \rightarrow 2^{+}_{2} \\ 2^{+}_{3} \rightarrow 2^{+}_{1} \\ 2^{+}_{3} \rightarrow 0^{+}_{1} \end{array}$	0.081(40)	62(36)	0.0581(27) 0.0340(17)	$78(13)$ $34(6)^a$	1693	36	1708	52
		$2_3^+ \rightarrow 4_1^+$	0.151(8)	5.6(8)	0.119(5)	4.0(7)		$\frac{4.5}{1}$		21 17
		$2_3^+ \to 2_2^+ \ 2_3^+ \to 2_1^+$	0.119(7) $0.235(13)$	3.5(7) $0.61(7)$	0.114(5) $0.225(9)$	3.1(5) $0.54(9)$		0.02		0.03
		$2_3^+ \to 0_1^+$	0.415(19)	0.315(49)	0.450(17)	*		0.07		0.04
0_{3}^{+}	1690	$0_3^+ \to 2_2^+ \ 0_3^+ \to 2_1^+$	0.138 $0.862(19)$	18.5(17) 11.9(17)	0.072(4) 0.928(4)	9.2(15) *	1570	15 13		$\frac{44}{2.2}$
2_4^+	1979	$\begin{array}{c} 2_{4}^{+} \rightarrow 0_{3}^{+} \\ 2_{4}^{+} \rightarrow 4_{2}^{+} \\ 2_{4}^{+} \rightarrow 0_{2}^{+} \end{array}$		5 - 68	0.0079(9) 0.0048(4) 0.0147(13)	53(12) 1.4(3) 1.12(23)	2146	33		49
		$\begin{array}{c} 2_{4}^{+} \rightarrow 3_{1}^{+} \\ 2_{4}^{+} \rightarrow 4_{1}^{+} \end{array}$	0.100(0.1)	4 4 7 (2.2)	0.0138(12)	$0.90(19)^a$				
		$2_4^+ \rightarrow 4_1^+$	0.183(34)	1.47(38)	0.262(9)	2.2(4)		6.4		1.4
		$2_4^{\stackrel{+}{+}} \rightarrow 2_2^{\stackrel{+}{+}}$	0.38(5)	2.7(8)	0.361(11)	2.6(5)		4.4		3.3
		$2_4^+ \to 2_1^+ \\ 2_4^+ \to 0_1^+$	0.183(45) $0.25(5)$	$0.21(7) \\ 0.11(2)$	0.090(5) $0.245(9)$	0.11(2)		$0.15 \\ 0.10$		$0.05 \\ 0.03$

 $^{a}B(E2)$ calculated assuming a pure E2 transition.

the peak intensity by the total intensity out of the level of interest [24, 25].

Shown in Fig. 2 is a partial level scheme for 124 Xe obtained from the current work, focusing on the decays of the 2^+_3 and 2^+_4 levels, and the results are listed in Table I. The coincidence spectrum of the 915-keV $0^+_2 \rightarrow 2^+_1 \gamma$ ray, shown in Fig. 3, clearly displays the 360-keV $2^+_3 \rightarrow 0^+_2 \gamma$ ray. The observed branch was 5.81(27)%, in agreement with the previously measured branch of 6.4(7)% [16], and the most recent measurement in the Coulomb excitation experiment [17] of 8(4)%. Figure 4 displays a portion of the coincidence spectrum with the 1336-keV $0^+_3 \rightarrow 2^+_1 \gamma$ ray, revealing the heretofore unobserved 289-keV transition from the 1979-keV 2^+_4 level. As can be seen, while the γ -ray peak is small, it is clearly present and the branching ratio extracted is 0.79(9)%.

The B(E2) values for the transitions were determined using ratios with previously measured B(E2) values for transitions from the same level determined via Coulomb excitation [17] via

$$B(E2) = B(E2)_{ref} \frac{E_{\gamma_{ref}}^5}{E_{\gamma}^5} \frac{BR}{BR_{ref}}$$
 (2)

where the subscript ref denotes the reference transition, and BR refers to the branching ratio. While the modification of the branching ratios and the observation of ad-

ditional transitions affect the Coulomb excitation yield, the population of any given level is largely determined by its direct feeding from the ground state, or in the case of levels with no measurable yield to ground state, from the 2_1^+ level. To verify this assumption, new calculations using the GOSIA code [27] were undertaken using the same assumptions as the original analysis [17] (since the system of equations is under-determined, the signs of the matrix elements were taken from an IBM calculation [17]) but with the newly extracted branching ratios. It was determined that the population of the 2^+ levels was not significantly affected by the new branching ratios, and therefore the direct $B(E2; 0_1^+ \to 2^+)$ values from the original analysis [17] remained valid. The B(E2) value for the 360-keV $2_3^+ \to 0_2^+$ transition was thus determined to be 78(13) W.u. and that of the 289-keV $2_4^+ \to 0_3^+$ transition 53(12) W.u. These values agree with the previous values of 62(36) W.u. and 5–68 W.u., respectively, but are considerably more precise. The new values for the low-lying 0^+ and 2^+ levels are listed in Table I; the B(E2) transition used as the reference value in Eq. 2 is indicated by an asterisk under the present results.

The newly-determined in-band B(E2) values reveal that the excited $K^{\pi}=0^+$ bands have considerably more quadrupole collectivity than previously thought. The 0_2^+ band has approximately twice the in-band B(E2) value predicted from the IBM calculations of Ref. [17] (78 \pm 13

vs. 36 W.u.), and also larger than predicted in recent dynamic pairing-plus-quadrupole (DPPQ) model calculations [28], also listed in Table I. The results for the 0_3^+ band further indicate that its quadrupole collectivity, as implied by the B(E2) value of 53 ± 12 W.u., is similar to that of the ground-state band and considerably more than the IBM predictions (33 W.u.) [17], but in excellent agreement with the DPPQ model predictions [28]. Unfortunately, predictions of the two-proton transfer strength in the DPPQ model are unavailable.

With the increased precision for the B(E2) values for transitions involving the $K^{\pi}=0^+$ band heads, the Kumar-Cline sum rules [29] can be used to extract the rotationally-invariant E2 moments via

$$\frac{1}{\sqrt{5}}Q^2 = \sum_{i} \langle 0 || \mathcal{M}(E2) || 2_i \rangle \langle 2_i || \mathcal{M}(E2) || 0 \rangle \begin{cases} 2 & 2 & 0 \\ 0 & 0 & 2 \end{cases}$$
(3)

where $\mathcal{M}(E2)$ is the transition matrix element and $\{\}$ is a 6j symbol. While the sum extends over the complete set of 2^+ states, it generally is determined by a few key matrix elements. The Q^2 invariant can be related to the β_0 shape parameter within the axially-symmetric rotational model via

$$Q^2 = q_0^2 \beta_0^2 \tag{4}$$

with $q_0 = \frac{3}{4\pi} Z R_0^2$ with $R_0 = 1.2 A^{\frac{1}{3}}$ fm. The values of β_0 determined using the present data given in Table I are listed in Table II together with the values predicted by the IBM [17] and DPPQ model [28]. In principle, the experimental values represent lower limits, but are unlikely to change significantly by extending the sum over more states. The conclusions reached regarding the degree of deformation of the 0^+ bands through the use

TABLE II. Values of β_0 extracted using Eqs. 3 and 4. For comparison, the corresponding values from the IBM calculations [17] and DPPQ model [28] are listed.

	Exp.	IBM	DPPQ
$\beta(0_1^+)$	0.227(3)	0.224	0.231
$\beta(0_2^+)$	0.29(2)	0.217	0.406
$\beta(0_3^+)$	0.22(2)	0.182	0.286

of quadrupole invariants are consistent with the expectations from the magnitude of the in-band $B(E2; 2^+ \to 0^+)$ values; the 0_2^+ band has significantly greater quadrupole collectivity than the ground state, and the 0_3^+ band has an equal degree within uncertainty.

The observation of similar quadrupole collectivity for the low-lying fragment of the proton-pairing vibration as observed for the ground state in ¹²⁴Xe provides a constraint on nuclear structure models used in this region. As shown in Table II, for the excited 0⁺ states the IBM predicts that β_0 decreases, whereas the DPPQ predicts an excessive deformation. (Models typically fit the $B(E2; 2_1^+ \to 0_1^+)$ value, thus agreement for $\beta(0_1^+)$ is to be expected.) The present work, which measured the branching ratios of γ rays, is insufficient to determine if the excited bands are prolate or oblate, only that the 0_2^+ band has a larger β_0 value than the ground state, and that of the 0_3^+ band is essentially identical. Detailed spectroscopic measurements of this type are required for the heavier Xe and Te isotopes, especially for those used in experimental searches for neutrinoless double- β decay.

This work was supported in part by the Natural Sciences and Engineering Research Council (Canada), TRI-UMF through the National Research Council (Canada), and by the U.S. National Science Foundation under Grant No. PHY-0956310.

^[1] D.J. Rowe and J.L. Wood, Fundamentals of Nuclear Models, (World Scientific, Singapore, 2010).

P. Vogel, J. Phys. G: Nucl. Part. Phys. 39, 124002 (2012).

^[3] D.R. Artusa et al., Adv. High Energy Phys. 2014, 878971 (2014).

^[4] M. Auger et al., Phys. Rev. Lett. 109, 032505 (2012).

^[5] M.I. Krivoruchenko et al., Nucl. Phys. A859, 140 (2011).

^[6] J. Suhonen, J. Phys. G: Nucl. Part. Phys. 40, 075102 (2013).

^[7] S.J. Freeman and J.P. Schiffer, J. Phys. G: Nucl. Part. Phys. 39, 124004 (2012).

^[8] H.W. Fielding et al., Nucl. Phys. A281, 389 (1977).

^[9] R.A. Meyer and L. Peker, Z. Phys. A 283, 379 (1977).

^[10] K. Heyde et al., Phys. Rev. C 25, 3160 (1982).

^[11] J. Kumpulainen *et al.*, Phys. Rev. C **45**, 640 (1992).

^[12] M. Délèze et al., Nucl. Phys. A551, 269 (1993).

^[13] H.W. Fielding et al., Nucl. Phys. **A304**, 520 (1978).

^[14] A.V. Afanasjev et al., Phys. Rep. **322**, 1 (1999).

^[15] W.P. Alford et al., Nucl. Phys. A323, 339 (1979).

 ^[16] K. Kitao et al., Nucl. Data Sheets 96, 241 (2002); T. Tamura, ibid. 108, 455 (2007); J. Katakura and Z.D.

Wu, *ibid.* **109**, 1655 (2008); J. Katakura and K. Kitao, *ibid.*, **97**, 765 (2002); M. Kanbe and K. Kitao, *ibid.* **94**, 227 (2001); B. Singh, *ibid.* **93**, 33 (2001).

^[17] G. Rainovski et al., Phys. Lett. **B683**, 11 (2010).

^[18] L. Coquard et al., Phys. Rev. C 83, 044318 (2011).

^[19] K. Heyde and J.L. Wood, Rev. Mod. Phys. 83, 1467 (2011).

^[20] L. Coquard et al., Phys. Rev. C 80, 061304(R) (2009).

^[21] L. Coquard et al., Phys. Rev. C 82, 024317 (2010).

^[22] A.B. Garnsworthy and P.E. Garrett, Hyp. Int. 225, 121 (2014).

^[23] D.C. Radford, http://radware.phy.ornl.gov.

^[24] P.E. Garrett et al., Phys. Rev. C 86, 044304 (2012).

^[25] A.J. Radich et al., Proc. of the Conf. Advances in Radioactive Isotope Science 2014, JPS Conf. Proc. (in press) (2015).

^[26] W.D. Kulp et al., Phys. Rev. C 76, 034319 (2007).

^[27] T. Czosnyka et al., Bull. Am. Phys. Soc. 28 745 (1983).

^[28] J.B. Gupta, Nucl. Phys. **A927**, 53 (2014).

^[29] D. Cline, Ann. Rev. Nucl. Part. Sci. 36, 683 (1986).